Precise Measurement of *B* Meson Lifetimes with Hadronic Decay Final States

K. Abe,[9] K. Abe,[42] R. Abe,[31] T. Abe,[43] I. Adachi,[9] Byoung Sup Ahn,[17] H. Aihara,[44] M. Akatsu,[24] Y. Asano,[49] T. Aso,[48] T. Aushev,[14] A. M. Bakich,[39] Y. Ban,[35] E. Banas,[29] S. Behari,[9] P. K. Behera,[50] A. Bondar,[2] A. Bozek,[29] J. Brodzicka,[29] T. E. Browder,[8] B. C. K. Casey,[8] P. Chang,[28] Y. Chao,[28] B. G. Cheon,[38] R. Chistov,[14] S.-K. Choi,[7] Y. Choi,[38] L. Y. Dong,[12] J. Dragic,[23] A. Drutskoy,[14] S. Eidelman,[2] V. Eiges,[14] Y. Enari,[24] C. W. Everton,[23] F. Fang,[8] H. Fujii,[9] C. Fukunaga,[46] M. Fukushima,[11] N. Gabyshev,[9] A. Garmash,[2,9] T. Gershon,[9] A. Gordon,[23] H. Guler,[8] R. Guo,[26] J. Haba,[9] H. Hamasaki,[9] K. Hanagaki,[36] F. Handa,[43] K. Hara,[33] T. Hara,[33] N. C. Hastings,[23] H. Hayashii,[25] M. Hazumi,[9] E. M. Heenan,[23] I. Higuchi,[43] T. Higuchi,[44] T. Hokuue,[24] Y. Hoshi,[42] S. R. Hou,[28] W.-S. Hou,[28] S.-C. Hsu,[28] H.-C. Huang,[28] T. Igaki,[24] Y. Igarashi,[9] T. Iijima,[9] H. Ikeda,[9] K. Inami,[24] A. Ishikawa,[24] H. Ishino,[45] R. Itoh,[9] H. Iwasaki,[9] Y. Iwasaki,[9] H. K. Jang,[37] J. H. Kang,[53] J. S. Kang,[17] P. Kapusta,[29] N. Katayama,[9] H. Kawai,[3] H. Kawai,[44] Y. Kawakami,[24] N. Kawamura,[1] T. Kawasaki,[31] H. Kichimi,[9] D. W. Kim,[38] Heejong Kim,[53] H. J. Kim,[53] H. O. Kim,[38] Hyunwoo Kim,[17] S. K. Kim,[37] T. H. Kim,[53] K. Kinoshita,[5] H. Konishi,[47] S. Korpar,[22,15] P. Križan,[21,15] P. Krokovny,[2] R. Kulasiri,[5] S. Kumar,[34] A. Kuzmin,[2] Y.-J. Kwon,[53] J. S. Lange,[6] S. H. Lee,[37] A. Limosani,[23] D. Liventsev,[14] R.-S. Lu,[28] J. MacNaughton,[13] G. Majumder,[40] F. Mandl,[13] D. Marlow,[36] T. Matsubara,[44] T. Matsuishi,[24] S. Matsumoto,[4] T. Matsumoto,[24] Y. Mikami,[43] W. Mitaroff,[13] K. Miyabayashi,[25] Y. Miyabayashi,[24] H. Miyake,[33] H. Miyata,[31] G. R. Moloney,[23] S. Mori,[49] T. Mori,[4] T. Nagamine,[43] Y. Nagasaka,[10] Y. Nagashima,[33] T. Nakadaira,[44] E. Nakano,[32] M. Nakao,[9] J. W. Nam,[38] Z. Natkaniec,[29] K. Neichi,[42] S. Nishida,[18] O. Nitoh,[47] S. Noguchi,[25] T. Nozaki,[9] S. Ogawa,[41] F. Ohno,[45] T. Ohshima,[24] T. Okabe,[24] S. Okuno,[16] S. L. Olsen,[8] W. Ostrowicz,[29] H. Ozaki,[9] P. Pakhlov,[14] H. Palka,[29] C. S. Park,[37] C. W. Park,[17] H. Park,[19] K. S. Park,[38] L. S. Peak,[39] J.-P. Perroud,[20] M. Peters,[8] L. E. Piilonen,[51] J. L. Rodriguez,[8] F. Ronga,[20] M. Rozanska,[29] K. Rybicki,[29] H. Sagawa,[9] Y. Sakai,[9] M. Satapathy,[50] A. Satpathy,[9,5] O. Schneider,[20] S. Schrenk,[5] C. Schwanda,[9,13] S. Semenov,[14] K. Senyo,[24] M. E. Sevior,[23] H. Shibuya,[41] B. Shwartz,[2] V. Sidorov,[2] J. B. Singh,[34] S. Stanič,[49] A. Sugi,[24] A. Sugiyama,[24] K. Sumisawa,[9] T. Sumiyoshi,[9] K. Suzuki,[9] S. Suzuki,[52] S. Y. Suzuki,[9] H. Tajima,[44] T. Takahashi,[32] F. Takasaki,[9] M. Takita,[33] K. Tamai,[9] N. Tamura,[31] J. Tanaka,[44] M. Tanaka,[9] G. N. Taylor,[23] Y. Teramoto,[32] S. Tokuda,[24] M. Tomoto,[9] T. Tomura,[44] S. N. Tovey,[23] K. Trabelsi,[8] T. Tsuboyama,[9] T. Tsukamoto,[9] S. Uehara,[9] K. Ueno,[28] Y. Unno,[3] S. Uno,[9] Y. Ushiroda,[9] K. E. Varvell,[39] C. C. Wang,[28] C. H. Wang,[27] J. G. Wang,[51] M.-Z. Wang,[28] Y. Watanabe,[45] E. Won,[37] B. D. Yabsley,[9] Y. Yamada,[9] M. Yamaga,[43] A. Yamaguchi,[43] H. Yamamoto,[43] Y. Yamashita,[30] M. Yamauchi,[9] S. Yanaka,[45] J. Yashima,[9] M. Yokoyama,[44] Y. Yuan,[12] Y. Yusa,[43] C. C. Zhang,[12] J. Zhang,[49] Y. Zheng,[8] V. Zhilich,[2] and D. Žontar[49]

(Belle Collaboration)

[1]*Aomori University, Aomori*
[2]*Budker Institute of Nuclear Physics, Novosibirsk*
[3]*Chiba University, Chiba*
[4]*Chuo University, Tokyo*
[5]*University of Cincinnati, Cincinnati, Ohio*
[6]*University of Frankfurt, Frankfurt*
[7]*Gyeongsang National University, Chinju*
[8]*University of Hawaii, Honolulu, Hawaii*
[9]*High Energy Accelerator Research Organization (KEK), Tsukuba*
[10]*Hiroshima Institute of Technology, Hiroshima*
[11]*Institute for Cosmic Ray Research, University of Tokyo, Tokyo*
[12]*Institute of High Energy Physics, Chinese Academy of Sciences, Beijing*
[13]*Institute of High Energy Physics, Vienna*
[14]*Institute for Theoretical and Experimental Physics, Moscow*
[15]*J. Stefan Institute, Ljubljana*
[16]*Kanagawa University, Yokohama*
[17]*Korea University, Seoul*
[18]*Kyoto University, Kyoto*
[19]*Kyungpook National University, Taegu*
[20]*IPHE, University of Lausanne, Lausanne*
[21]*University of Ljubljana, Ljubljana*
[22]*University of Maribor, Maribor*
[23]*University of Melbourne, Victoria*
[24]*Nagoya University, Nagoya*

 0031-9007/02/88(17)/171801(6)$20.00

[25]Nara Women's University, Nara
[26]National Kaohsiung Normal University, Kaohsiung
[27]National Lien-Ho Institute of Technology, Miao Li
[28]National Taiwan University, Taipei
[29]H. Niewodniczanski Institute of Nuclear Physics, Krakow
[30]Nihon Dental College, Niigata
[31]Niigata University, Niigata
[32]Osaka City University, Osaka
[33]Osaka University, Osaka
[34]Panjab University, Chandigarh
[35]Peking University, Beijing
[36]Princeton University, Princeton, New Jersey
[37]Seoul National University, Seoul
[38]Sungkyunkwan University, Suwon
[39]University of Sydney, Sydney, New South Wales
[40]Tata Institute for Fundamental Research, Bombay
[41]Toho University, Funabashi
[42]Tohoku Gakuin University, Tagajo
[43]Tohoku University, Sendai
[44]University of Tokyo, Tokyo
[45]Tokyo Institute of Technology, Tokyo
[46]Tokyo Metropolitan University, Tokyo
[47]Tokyo University of Agriculture and Technology, Tokyo
[48]Toyama National College of Maritime Technology, Toyama
[49]University of Tsukuba, Tsukuba
[50]Utkal University, Bhubaneswer
[51]Virginia Polytechnic Institute and State University, Blacksburg, Virginia
[52]Yokkaichi University, Yokkaichi
[53]Yonsei University, Seoul

(Received 1 February 2002; published 15 April 2002)

The lifetimes of the $\overline{B}^0$ and B^- mesons are extracted from 29.1 fb^{-1} of data collected with the Belle detector at the KEK B factory. A fit to the decay length differences of neutral and charged B meson pairs, measured in events where one of the B mesons is fully reconstructed in several hadronic modes, yields $\tau_{\overline{B}^0} = 1.554 \pm 0.030(\text{stat}) \pm 0.019(\text{syst})$ ps, $\tau_{B^-} = 1.695 \pm 0.026(\text{stat}) \pm 0.015(\text{syst})$ ps, and $\tau_{B^-}/\tau_{\overline{B}^0} = 1.091 \pm 0.023(\text{stat}) \pm 0.014(\text{syst})$.

DOI: 10.1103/PhysRevLett.88.171801 PACS numbers: 13.25.Hw, 12.39.Hg

Lifetime measurements of $\overline{B}^0$ and B^- provide key input to the determination of the Kobayashi-Maskawa matrix element $|V_{cb}|$ [1]. Moreover, the ratio of the lifetimes is sensitive to effects beyond the spectator model. In the framework of heavy quark expansion, the B lifetime ratio is predicted to be equal to one, up to small corrections proportional to $1/m_b^3$ [2], where m_b is the mass of the b quark. A recent theoretical study predicts $\tau_{B^-}/\tau_{\overline{B}^0} = 1.07 \pm 0.03$ [3], which agrees with the world average of measurements, $\tau_{B^-}/\tau_{\overline{B}^0} = 1.073 \pm 0.027$ [4]. The *BABAR* Collaboration recently reported $\tau_{B^-}/\tau_{\overline{B}^0} = 1.082 \pm 0.026 \pm 0.012$ [5]. Accurate determinations of the $\overline{B}^0$ and B^- lifetimes also provide essential input to analyses of CP violation and neutral B mixing.

The analysis described here is based on a 29.1 fb^{-1} data sample, which contains 31.3×10^6 $B\overline{B}$ pairs, collected with the Belle detector [6] at the asymmetric-energy KEKB collider (8.0 GeV electrons against 3.5 GeV positrons) [7]. Electron-positron annihilations produce $\Upsilon(4S)$ mesons moving along the electron beam line (z axis) with $(\beta\gamma)_\Upsilon = 0.425$, and decaying into $B^0\overline{B}^0$ or B^+B^-. Since the B mesons are nearly at rest in the $\Upsilon(4S)$ center of mass system (cms), B lifetimes can be determined from the separation in z between the two B decay vertices. The average separation is $c\tau_B(\beta\gamma)_\Upsilon \sim 200$ μm, where τ_B is the B meson lifetime. In this analysis, one of the B decay vertices is determined from a fully reconstructed B meson, while the other is determined inclusively using the rest of the tracks in the event.

The Belle detector consists of a three-layer silicon vertex detector (SVD), a 50-layer central drift chamber (CDC), an array of 1188 aerogel Cherenkov counters (ACC), 128 time-of-flight (TOF) scintillation counters, an electromagnetic calorimeter containing 8736 CsI(Tl) crystals (ECL), and 14 layers of 4.7-cm-thick iron plates interleaved with a system of resistive plate counters (KLM). All subdetectors except the KLM are located inside a 3.4 m diam superconducting solenoid which provides a 1.5 T magnetic field. The impact parameter resolutions for charged tracks are measured to be $\sigma_{xy}^2 = (19)^2 + [50/(p\beta \times \sin^{3/2}\theta)]^2$ μm^2 in the plane perpendicular to the z axis and $\sigma_z^2 = (36)^2 + [42/(p\beta\sin^{5/2}\theta)]^2$ μm^2 along the z axis, where $\beta = pc/E$, p and E are the momentum (GeV/c) and energy (GeV), and θ is the polar angle from the z axis. The transverse momentum resolution is $(\sigma_{p_t}/p_t)^2 = (0.0030/\beta)^2 + (0.0019 p_t)^2$, where p_t is in GeV/c.

$\overline{B}^0$ and B^- mesons are fully reconstructed in the following decay modes: $\overline{B}^0 \to D^+\pi^-$, $D^{*+}\pi^-$, $D^{*+}\rho^-$, $J/\psi K_S^0$, $J/\psi \overline{K}^{*0}$, $B^- \to D^0\pi^-$, and $J/\psi K^-$ [8].

Charged pion and kaon candidates are required to satisfy selection criteria based on particle-identification likelihood functions derived from specific ionization (dE/dx) in the CDC, time-of-flight, and the response of the ACC. Electrons are identified using a combination of dE/dx, the response of the ACC, and the position, shape, and total energy (i.e., E/p) of their associated ECL showers. Muon candidates must penetrate the iron plates of the KLM in a manner consistent with the muon hypothesis.

The reconstruction and selection criteria for $K_S^0 \to \pi^+\pi^-$ and $J/\psi \to \ell^+\ell^-$ ($\ell = e, \mu$) are described elsewhere [9]. $\overline{K}^{*0}$ candidates are reconstructed in the $\overline{K}^{*0} \to K^-\pi^+$ channel and required to have an invariant mass within 75 MeV/c^2 of the average $\overline{K}^{*0}$ mass.

Photon candidates are defined as isolated ECL clusters of more than 20 MeV that are not matched to any charged track. π^0 candidates are reconstructed from pairs of photon candidates with invariant masses between 124 and 146 MeV/c^2. A mass-constrained fit is performed to improve the π^0 momentum resolution. A minimum π^0 momentum of 0.2 GeV/c is required. ρ^- candidates are selected as $\pi^-\pi^0$ pairs having invariant masses within 150 MeV/c^2 of the average ρ^- mass.

Neutral and charged D candidates are reconstructed in the following channels: $D^0 \to K^-\pi^+$, $K^-\pi^+\pi^0$, $K^-\pi^+\pi^+\pi^-$, and $D^+ \to K^-\pi^+\pi^+$. $D^{*+} \to D^0\pi^+$ candidates are formed by combining a D^0 candidate with a slow and positively charged track, for which no particle identification is required.

To reduce continuum background, a selection based on the ratio of the second to zeroth Fox-Wolfram moments [10] and the angle between the thrust axes of the reconstructed and associated B mesons is applied mode by mode.

The decay vertices of the two B mesons in each event are fitted using tracks that are associated with at least one SVD hit in the r-ϕ plane and at least two SVD hits in the r-z plane under the constraint that they are consistent with the interaction point (IP) profile, smeared in the r-ϕ plane by 21 μm, to account for the transverse B decay length. The IP profile is described as a three-dimensional Gaussian, the parameters of which are determined in each run (every 60 000 events in case of the mean position) using hadronic events. The size of the IP region is typically $\sigma_x \simeq 100$ μm, $\sigma_y \simeq 5$ μm, and $\sigma_z \simeq 3$ mm, where x and y denote horizontal and vertical directions, respectively.

In the case of a fully reconstructed $\overline{B} \to D^{(*)}X$ decay, the B decay point is obtained from the vertex position and momentum vector of the reconstructed D meson and a track other than the slow π^+ candidate from D^{*+} decay. For a fully reconstructed $\overline{B} \to J/\psi X$ decay, the B vertex is determined using lepton tracks from the J/ψ. The decay vertex of the associated B meson is determined from tracks not assigned to the fully reconstructed B meson; however, poorly reconstructed tracks (with a longitudinal position error in excess of 500 μm) as well as tracks likely to come from K_S^0 decays (forming the K_S^0 mass with another track, or more than 500 μm away from the fully reconstructed B vertex in the r-ϕ plane) are not used.

The quality of the fit is assessed only in the z direction (because of the tight IP constraint in the transverse plane), using the following variable $\xi \equiv (1/2n)\sum_i^n[(z^i_{\rm after} - z^i_{\rm before})/\varepsilon^i_{\rm before}]^2$, where n is the number of tracks used in the fit, $z^i_{\rm before}$ and $z^i_{\rm after}$ are the z positions of each track (at the closest approach to the origin) before and after the vertex fit, respectively, and $\varepsilon^i_{\rm before}$ is the error of $z^i_{\rm before}$. A Monte Carlo (MC) study shows that ξ does not depend on the B decay length. We require $\xi < 100$ to eliminate poorly reconstructed vertices. About 3% of the fully reconstructed and 1% of the associated B decay vertices are rejected.

The proper-time difference between the fully reconstructed and the associated B decays, $\Delta t \equiv t_{\rm rec} - t_{\rm asc}$, is calculated as $\Delta t = (z_{\rm rec} - z_{\rm asc})/[c(\beta\gamma)_\Upsilon]$, where $z_{\rm rec}$ and $z_{\rm asc}$ are the z coordinates of the fully reconstructed and associated B decay vertices, respectively. We reject a small fraction ($\sim$0.2%) of the events by requiring $|\Delta t| < 70$ ps ($\sim 45\tau_B$). The final event selection is based on requirements on the energy difference $\Delta E \equiv E_B^{\rm cms} - E_{\rm beam}^{\rm cms}$ and the beam-energy constrained mass $M_{\rm bc} \equiv \sqrt{(E_{\rm beam}^{\rm cms})^2 - (p_B^{\rm cms})^2}$, where $E_{\rm beam}^{\rm cms}$, $E_B^{\rm cms}$, and $p_B^{\rm cms}$ are the beam energy, the energy, and the momentum of the fully reconstructed B candidate in the cms, respectively. If more than one fully reconstructed B candidate is found in the same event, the one with the best χ^2 for ΔE and $M_{\rm bc}$ (and the invariant mass of the D candidate for the $\overline{B} \to D^{(*)}X$ case) is chosen. For each channel, a square signal region is defined in the ΔE-$M_{\rm bc}$ plane, corresponding to $\pm 3\sigma$ windows centered on the expected means for ΔE and $M_{\rm bc}$. A standard deviation is about 3 MeV/c^2 for $M_{\rm bc}$ and 10–30 MeV for ΔE depending on the decay mode. After all vertexing and selection requirements, we find 7863 $\overline{B}^0$ and 12 047 B^- events in the ΔE-$M_{\rm bc}$ signal region. Figure 1 shows the $M_{\rm bc}$ distributions for all the $\overline{B}^0$ and B^- candidates found in the ΔE signal region.

We extract lifetime information using an unbinned maximum likelihood fit to the observed Δt distributions. We maximize the likelihood function $L = \prod_i P(\Delta t_i)$, where $P(\Delta t)$ is the probability density function (PDF) for the proper-time difference Δt for each event and the product is taken over all selected events. The function $P(\Delta t)$, expressed as

$$P(\Delta t) = (1 - f_{\rm ol})[f_{\rm sig}P_{\rm sig}(\Delta t) + (1 - f_{\rm sig})P_{\rm bkg}(\Delta t)] + f_{\rm ol}P_{\rm ol}(\Delta t), \quad (1)$$

contains contributions from the signal and the background ($P_{\rm sig}$ and $P_{\rm bkg}$), where $P_{\rm sig}$ is described as the convolution

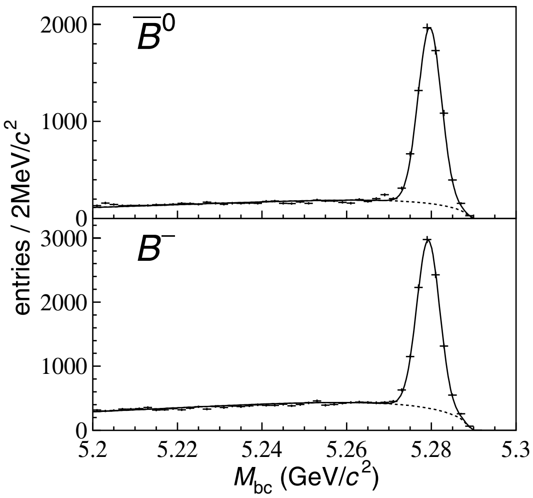

FIG. 1. The beam-energy constrained mass distributions of the fully reconstructed B candidates (neutral on top, charged on bottom). The dashed curves show the background contributions.

of a true PDF ($\mathcal{P}_{\rm sig}$) with a resolution function ($R_{\rm sig}$) and $P_{\rm bkg}$ is expressed in a similar way:

$$P_j(\Delta t) = \int_{-\infty}^{+\infty} d(\Delta t')\mathcal{P}_j(\Delta t')R_j(\Delta t - \Delta t'), \quad (2)$$

where $j = {\rm sig, bkg}$. To account for a small number of events that give large Δt in both the signal and background (outlier components), we add a third component: $P_{\rm ol}(\Delta t) = G(\Delta t; \sigma_{\rm ol})$, where $G(t;\sigma) \equiv \exp[-t^2/(2\sigma^2)]/(\sqrt{2\pi}\,\sigma)$ is the Gaussian function. The global fraction ($f_{\rm ol}$) and the width ($\sigma_{\rm ol}$) are left as free parameters in the fit.

The signal purity ($f_{\rm sig}$) is determined on an event-by-event basis as a function of ΔE and $M_{\rm bc}$. The two-dimensional distribution of these variables including the sideband region is fitted with the sum of a Gaussian signal function $F_{\rm sig}(\Delta E, M_{\rm bc})$ and a background function $F_{\rm bkg}(\Delta E, M_{\rm bc})$, represented as an ARGUS background function [11] in $M_{\rm bc}$ and a first-order polynomial in ΔE. The fraction of signal is then obtained as $f_{\rm sig}(\Delta E, M_{\rm bc}) = F_{\rm sig}/[F_{\rm sig} + F_{\rm bkg}]$. The true PDF for the signal is given by

$$\mathcal{P}_{\rm sig}(\Delta t) = \frac{1}{2\tau_B}\exp\left(-\frac{|\Delta t|}{\tau_B}\right), \quad (3)$$

where τ_B is, depending on the reconstructed mode in the event, either the $\overline{B}^0$ or the B^- lifetime. The resolution function of the signal is constructed as the convolution of four different contributions: the detector resolutions on $z_{\rm rec}$ and $z_{\rm asc}$ ($R_{\rm rec}$and $R_{\rm asc}$), an additional smearing on $z_{\rm asc}$ due to the inclusion of tracks which do not originate from the associated B vertex ($R_{\rm np}$), mostly due to charm and K_S decays, and the kinematic approximation that the B mesons are at rest in the cms ($R_{\rm k}$).

For a vertex obtained from multiple tracks, $R_{\rm rec}$ and $R_{\rm asc}$ are parametrized as a single Gaussian function, $G(t; (s_j^0 + s_j^1\xi_j)\sigma_j)$ ($j = {\rm rec, asc}$) where σ_j is the proper-time error estimated vertex by vertex from the z_j error, and $(s_j^0 + s_j^1\xi_j)$ is a scale factor based on the vertex fit quality ξ defined above. The parameters for the scale factor, $s_j^{0,1}$, are determined from the lifetime fit. The typical value of the scale factor is 1.32 for $R_{\rm rec}$ and 1.20 for $R_{\rm asc}$. For a vertex obtained from a single track [12], we use $(1 - f_{\rm tail}) \times G(t; s_{\rm main}\sigma_j) + f_{\rm tail}G(t; s_{\rm tail}\sigma_j)$, where $s_{\rm main}$ and $s_{\rm tail}$ are global scaling factors. The shape of $R_{\rm np}$ is determined from MC data sample, separately for $\overline{B}^0$ and B^- events. $R_{\rm k}$ is calculated analytically as a function of $E_B^{\rm cms}$ and $\cos\theta_B^{\rm cms}$ from the kinematics of the $\Upsilon(4S)$ two-body decay, where $\theta_B^{\rm cms}$ is the polar angle of the reconstructed B in the cms. The resulting Δt resolution for the signal is $\sim$1.56 ps (rms).

The background PDF, $P_{\rm bkg}(\Delta t)$, is modeled as a sum of exponential and prompt components convoluted with

$$R_{\rm bkg}(\Delta t) = (1 - f_{\rm tail}^{\rm bkg})G(\Delta t; s_{\rm main}^{\rm bkg}\sqrt{\sigma_{\rm rec}^2 + \sigma_{\rm asc}^2}\,) + f_{\rm tail}^{\rm bkg}G(\Delta t; s_{\rm tail}^{\rm bkg}\sqrt{\sigma_{\rm rec}^2 + \sigma_{\rm asc}^2}\,).$$

Different values are used for $s_{\rm main}^{\rm bkg}$, $s_{\rm tail}^{\rm bkg}$, and $f_{\rm tail}^{\rm bkg}$ depending on whether both vertices are reconstructed with multiple tracks or not. The parameters for the background function $P_{\rm bkg}$ are determined using the ΔE-$M_{\rm bc}$ sideband region for each decay mode. A MC study shows that the fraction of prompt component in the signal region is smaller (by $\sim$10%–50% depending on the decay mode) than that in the sideband region. We correct $P_{\rm bkg}$ for this effect.

In the final fit to the events in the signal region, we determine simultaneously twelve parameters: the $\overline{B}^0$ and B^- lifetimes, seven parameters for $R_{\rm rec}$ and $R_{\rm asc}$, and three parameters for the outlier component. We find $\sigma_{\rm ol} = 36^{+5}_{-4}$ ps, and $f_{\rm ol} = (0.06^{+0.03}_{-0.02})$% or (3.1 ± 0.4)% (multiple- or single-track case). The lifetime ratio, $r \equiv \tau_{B^-}/\tau_{\overline{B}^0}$, is obtained by repeating the final fit after replacing τ_{B^-} with $r\tau_{\overline{B}^0}$. The fit yields $\tau_{\overline{B}^0} = 1.554 \pm 0.030$ ps, $\tau_{B^-} = 1.695 \pm 0.026$ ps, and $\tau_{B^-}/\tau_{\overline{B}^0} = 1.091 \pm 0.023$. Figure 2 shows the distributions of Δt for $\overline{B}^0$ and B^- events in the signal region with the fitted curves superimposed.

The systematic errors are summarized in Table I. The systematic error due to the IP constraint is estimated by varying ($\pm$10 μm) the smearing used to account for the transverse B decay length. The IP profile is determined using two different methods and we find no change in the lifetime results. Possible systematic effects due to the track quality selection of the associated B decay vertices are studied by varying each criterion by 10%. The fit quality criterion for reconstructed vertices is varied from $\xi < 50$ to $\xi < 200$. We estimate the systematic uncertainty due to the maximum $|\Delta t|$ requirement by varying the $|\Delta t|$ range by $\pm$30 ps and taking the maximum excursion to be the systematic error. We examine the uncertainty in the scale of Δt arising from the measurement error of

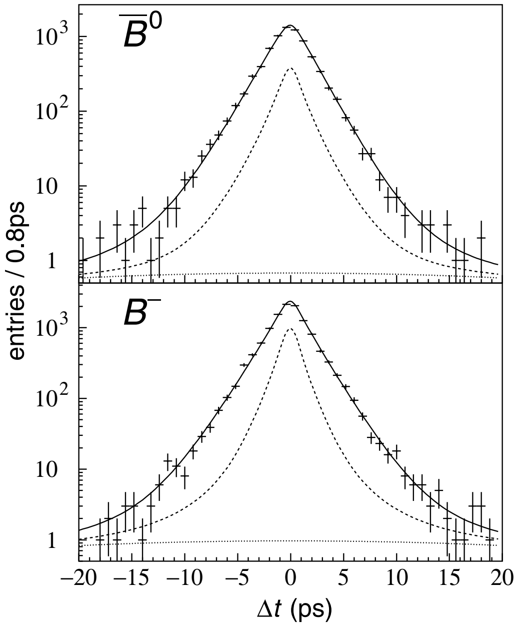

FIG. 2. The Δt distributions of neutral (top) and charged (bottom) B meson pairs, with fitted curves. The dashed lines represent the sum of the background and outlier component, and the dotted lines represent the outlier component.

the SVD sizes and thermal expansion during the operation, and find that its contribution to the lifetimes is negligibly small. ΔE-$M_{\rm bc}$ signal regions are varied by ± 10 MeV for ΔE and ± 3 MeV$/c^2$ for $M_{\rm bc}$. The parameters determining $f_{\rm sig}$ are varied by $\pm 1\sigma$ to estimate the associated systematic error. The systematic error due to the modeling of $R_{\rm sig}$ is estimated by comparing the results with different $R_{\rm sig}$ parametrizations. The lifetime fit is repeated after varying the $R_{\rm np}$ parameters by $\pm 2\sigma$. The lifetime dependence on the B meson mass, which is the input for $R_{\rm k}$, is measured by varying the mass by $\pm 1\sigma$ from the world average value and found the differences to be negligible. The systematic error due to the background shape is estimated by varying its parameters by their errors. The possible bias in the fitting procedure and the effect of SVD alignment error are studied with MC samples; we find no bias and include the MC statistics as a systematic error.

To conclude, we have presented new measurements of the $\overline{B}^0$ and B^- meson lifetimes using 29.1 fb^{-1} of data collected with the Belle detector near the $\Upsilon(4S)$ energy. Unbinned maximum likelihood fits to the distributions of the proper-time difference between the two B meson decays yield

$$\tau_{\overline{B}^0} = 1.554 \pm 0.030(\text{stat}) \pm 0.019(\text{syst})\ \text{ps},$$
$$\tau_{B^-} = 1.695 \pm 0.026(\text{stat}) \pm 0.015(\text{syst})\ \text{ps},$$
$$\tau_{B^-}/\tau_{\overline{B}^0} = 1.091 \pm 0.023(\text{stat}) \pm 0.014(\text{syst}).$$

These are currently the most precise measurements. A value of unity for $\tau_{B^-}/\tau_{\overline{B}^0}$ is ruled out at a level greater than 3σ and the measured value is consistent with the theoretical prediction [3].

TABLE I. Summary of systematic errors for neutral and charged B lifetimes, and their ratio. The errors are combined in quadrature.

	$\tau_{\overline{B}^0}$ (ps)	τ_{B^-} (ps)	$\tau_{B^-}/\tau_{\overline{B}^0}$
IP constraint	0.004	0.003	0.001
Track selection	0.006	0.004	0.001
Vertex selection	0.003	0.002	0.002
Δt range	0.003	0.002	0.001
ΔE-$M_{\rm bc}$ signal region	0.003	0.004	0.003
Signal fraction	0.001	0.001	0.001
$R_{\rm sig}$ parametrization	0.008	0.008	Cancels
$R_{\rm np}$ parameters	0.006	0.004	0.006
Background shape	0.012	0.007	0.011
MC statistics	0.006	0.007	0.005
Total	0.019	0.015	0.014

We wish to thank the KEKB accelerator group. We acknowledge support from the Ministry of Education, Culture, Sports, Science, and Technology of Japan and the Japan Society for the Promotion of Science; the Australian Research Council and the Australian Department of Industry, Science and Resources; the National Science Foundation of China under Contract No. 10175071; the Department of Science and Technology of India; the BK21 program of the Ministry of Education of Korea and the CHEP SRC program of the Korea Science and Engineering Foundation; the Polish State Committee for Scientific Research under Contract No. 2P03B 17017; the Ministry of Science and Technology of the Russian Federation; the Ministry of Education, Science and Sport of Slovenia; the National Science Council and the Ministry of Education of Taiwan; and the U.S. Department of Energy.

[1] M. Kobayashi and T. Maskawa, Prog. Theor. Phys. **49**, 652 (1973).
[2] I. Bigi, B. Blok, M. Shifman, N. Uraltsev, and A. Vainshtein, in *B Decays,* edited by S. Stone (World Scientific, Singapore, 1994), 2nd ed.; M. Neubert and C. T. Sachrajda, Nucl. Phys. **B483**, 339 (1997).
[3] D. Becirevic, in Proceedings of the International Europhysics Conference on High-Energy Physics, Budapest, 2001.
[4] Particle Data Group, D. E. Groom *et al.,* Eur. Phys. J. C **15**, 1 (2000); 2001 off year partial update for the 2002 edition available on the PDG WWW pages (http://pdg.lbl.gov).
[5] *BABAR* Collaboration, B. Aubert *et al.,* Phys. Rev. Lett. **87**, 201803 (2001).
[6] Belle Collaboration, A. Abashian *et al.,* Nucl. Instrum. Methods Phys. Res., Sect. A **479**, 117 (2002).
[7] KEKB *B* Factory Design Report, KEK Report No. 95-7, 1995 (unpublished).
[8] Throughout this paper, when a decay mode is quoted the inclusion of charge conjugate mode is implied.
[9] Belle Collaboration, A. Abashian *et al.,* Phys. Rev. Lett. **86**, 2509 (2001).
[10] G.C. Fox and S. Wolfram, Phys. Rev. Lett. **41**, 1581 (1978).

[11] ARGUS Collaboration, H. Albrecht *et al.,* Phys. Lett. B **241**, 278 (1990); the ARGUS function is presented as $ax\sqrt{1-(x/E_{\rm beam}^{\rm cms})^2}\exp\{b[1-(x/E_{\rm beam}^{\rm cms})^2]\}$, where a and b are constants that are determined from the data.

[12] The IP constraint enables us to determine a vertex even with a single track. The fraction of such vertices is about 1% for $z_{\rm rec}$ and 30% for $z_{\rm asc}$.